Wavefront correction of extended objects through image sharpness maximisation

L. P. Murray*, J. C. Dainty and J. Coignus†and F. Felberer‡

Applied Optics Group, Department of Experimental Physics, National University of Ireland, Galway, Ireland.

ABSTRACT

Many adaptive optics systems rely on a wavefront sensor (WFS) to sense the aberrations in an incoming wavefront. The required corrections are determined and applied by the wavefront corrector - often a deformable mirror (DM). We wish to develop a wavefront sensor-less correcting system, as derived from the original adaptive optics system of Muller and Buffington[1]. In this experiment we apply commands to a corrective element with adjustable segments in an attempt to maximise a metric which correlates to image quality. We employ search algorithms to find the optimal combination of actuator voltages on a DM to maximise a certain sharpness metric. The "sharpness" is based on intensity measurements taken with a CCD camera. It has shown [2] that sharpness maximisation, using the Simplex algorithm[3], can minimise the aberrations and restore the Airy rings of an imaged point source. The results are repeatable and so-called "blind" correction of the aberrations is achieved. This paper demonstrates that the technique can be applied to extended objects which have been aberated using a Hamamatsu SLM to induce aberrations. The correction achieved using various search algorithms are evaluated and presented.

Keywords: Adaptive Optics, Image Sharpness, Simplex Algorithm

1. INTRODUCTION

In conventional adaptive optics (AO) systems a deformable mirror (DM) is used to correct for an incoming aberrated wavefront. The necessary corrections that need to be applied to the deformable mirror are determined using a WFS. These corrections are applied to the DM through a control computer. This vast area affected and dependant on adaptive optics stems originally from an AO system proposed by H. Babcock[3]. The corrections to be applied conventionally rely on the use of a WFS which measure the phase, phase gradient or phase curvature directly[4,5,6]. It is shown that wavefront-sensorless correction can be made to aberrated images in a simple regime.

1.1. Wavefront Sensing

The area of wavefront sensing can be broken into to distinct groups. Indirect and direct wavefront sensing. In direct WFS a wavefront sensor is required to sense the wavefront with high spatial resolution and speed to apply realtime correction. Direct methods provide information about wavefront phase and this information is used to drive a wavefront corrector. Generally direct methods are employed in atmospheric and visions science where correction need to be made at a higher rate.

The wavefront sensor is one of the basic elements of conventional adaptive optics systems. Wavefront measurements need to be fast, and with a high spatial resolution. Indeed, for real-time corrections, measurement and deformable mirror adaptation have to last less than the typical constant time of atmospheric distortions changes. Direct wavefront sensing methods such as the Shack-Hartmann WFS[4] provide information about the wavefront phase, which is then used drive a wavefront corrector. In this sense, direct wavefront sensors directly measure the wavefront phase from which the necessary correction can be determined.

Indirect techniques do not directly measure implicit or explicit wavefront properties, but use information related to the wavefront to provide the signal for the corrective element without reconstruction. This area of research is based on a "sharpness" criterion, which is used as an image metric to measure the degree of correction of the wavefront phase. The principle of image sharpening can be explained by figure 1, a schematic diagram of image sharpening methods.

*Further information: (Send correspondence to L. P. M.) E-mail: larry.murray@nuigalway.ie, Telephone +353 91 492428
†ENSPG, Grenoble, France, j.coignus@yahoo.fr
‡Vienna University of Technology, Austria, franzf@iaste.at

5th International Workshop on Adaptive Optics for Industry and Medicine, edited by Wenhan Jiang,
Proc. of SPIE Vol. 6018, 60181A, (2005) · 0277-786X/05/$15 · doi: 10.1117/12.669380

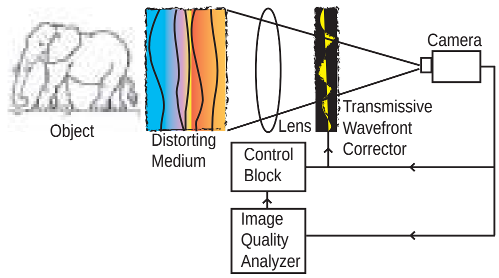

Figure 1. Basic configuration of image sharpness correction system (after Vorontsov[8])

The image sharpness metric is a measure of the image quality and in general the higher this metric the better the image quality. In sharpness maximisation a trial phase correction is applied to the image via a corrector and the effect on the sharpness metric is noted. Using a suitable sharpness metric, and a search algorithm which determines the trial phase to be applied to the corrector, the system is driven to maximise the sharpness metric and minimise the aberration.

2. IMAGE SHARPNESS PRINCIPLE

The concept of correcting for aberrations in an optics system based on image metrics was first proposed by Muller and Buffington in 1974[1]. This method uses a definition of sharpness of image to minimize aberrations in conjunction with a wavefront correcting medium. This technique was superseded with the advent of modern day WFS such as the Shack-Hartmann due to the speed of correction that they facilitated. However, with increasing CCD camera speeds and computation powers of modern day computers this method can be used for slowly varying or static aberrations.

An image sharpness metric is a measure of image quality and in general the higher the metric the better the image quality. In sharpness maximisation a trial phase correction is applied via a corrector and the effect on sharpness is noted. Using a suitable sharpness metric and a search algorithm, which determines a trial phase to be applied to the wavefront corrector, the system is driven to maximise the sharpness metric and minimise the aberration.

The sharpness maximisation relies on how the sharpness is defined. The problem arises when one quantitatively tries to define the word “sharp”. Muller and Buffington define the sharpness such that its value for an aberration-degraded image is always less than that of the true image. In their paper Muller and Buffington set out 8 sharpness metrics, some of which have been proven to be maximised for various images. One such sharpness definition is

$$S_1 = \int I^n(x,y)dxdy \quad n = 2,3,4, \tag{1}$$

where x, y denote coordinates in the image plane and $I(x,y)$is the image irradiance. This sharpness definition will be maximised when there is zero wavefront error, even in the presence of irregular object radiance distribution. This amplitude insensitivity makes this method useful for large extended objects. Other sharpness functions, such as higher-order moments of distribution, or entropy minimization functions,

$$S_2 = -\int I(x,y)ln[I(x,y)]dxdy, \tag{2}$$

have been examined by Muller and Buffington[1] and are proven to relate to low wavefront error. Numerous papers have since been published detailing further image sharpness metrics[2]. Some metrics which have been developed are object dependant and the metric is chosen based on the scene[7-11]

3. SEARCH ALGORITHMS

Image sharpness maximisation requires the correcting device to be driven to its optimal shape to minimise the aberrations. For a DM with 37 actuators which operate over 255 different voltages this is an unfeasibly large space to search systematically. To search the large range of possible mirror shapes (255^{37}degrees of freedom (DOF)) it is necessary to implement a search algorithm to determine the global minimum.

Ideally when using a search algorithm routine the global minimum is the final state i.e. the true minimum of the system. This is very difficult to find for systems having a large number of DOF, due to the probability of falling into a local minimum. Generally, for complicated optimisation problems, non-systematic search routines, such as, the Nelder-Mead Simplex, Stochastic Gradient Descent (SGD), Stochastic Parallel Gradient Descent (SPGD), will give the best solution[12].

3.1. The Nelder-Mead Simplex Algorithm

The simplex search method proposed by Nelder and Mead[13] is an algorithm that tries to minimise a scalar-valued nonlinear function of n real variables using only function values. A simplex is a geometrical figure consisting of $n + 1$ vertices, where n is the number of DOF. In two dimensions a simplex would be a triangle, in three, a tetrahedron and in this experiment a complex figure with 38 vertices. Each vertex represents a set of mirror voltages. Initially, 38 $(n + 1)$ random sets of voltages are generated and the corresponding sharpness value is measured for each vertex. Based on the initial evaluations the simplex attempts to adapt to the local landscape, with the aim of contracting to the global minimum. This is done through a series of reflections, expansions, contractions and shrink operations. The simplex can be set to run for a certain number of iterations, or to stop when a termination criteria is met.

Although Nelder and Mead published their paper in 1965, no theoretical results regarding convergence properties of the Nelder-Mead method in higher dimensions have yet been proven. Even finding any function in R^2 for which the algorithm would always converge to a minimum still remains and open problem[14]. Therefore, one cannot say with certainty that the maximum sharpness value reached by the simplex is the global maximum.

3.2. Stochastic Gradient Descent Processes

This is an iterative multivariate optimisation search method, first implemented on an adaptive optics system by Vorontsov[15]. Stochastic methods add random processes which aid the algorithm to converge on the global maximum.

In standard gradient descent the true gradient is used to update the actuator voltages. The true gradient is usually the sum of the gradients caused by each individual trial perturbation. The voltages are adjusted by the negative of the true gradient multiplied by a step size. Therefore, standard gradient descent requires one sweep through the training set before any voltages can be changed.

In stochastic parallel gradient descent the true gradient is approximated by the gradient of the cost function only evaluated on a single trial perturbation. The voltages are then adjusted by an amount proportional to this approximate gradient. Therefore, the parameters of the algorithm are updated after each perturbation. For a large number of degrees of freedom stochastic parallel gradient descent is much faster that general gradient descent.

3.3. Simulated Annealing

Simulated annealing (SA) is a generic algorithm for the global optimization problem, namely locating a good approximation to the global optimum of a large search space. The name and inspiration come from annealing in metallurgy, a technique involving heating and controlled cooling of a material to increase the size of its crystals and reduce their defects. The heat causes the atoms to become unstuck from their initial positions (a local minimum of the internal energy) and wander randomly through states of higher energy; the slow cooling gives them more chances of finding configurations with a lower internal energy that the initial one.

In the simulated annealing method, each point in the search space is compared to a state of some physical system, and the function *E(s)* to be minimized is interpreted as the internal energy of the system in that state. Therefore the goal is to bring the system, from an arbitrary *initial* state, to a state with the minimum possible energy[16].

As recommend by Press at al[17] the new trial points for the SA algorithm are generated by incorporating a Simplex approach.

4. EXPERIMENTAL PROCEDURE

4.1. Apparatus

A narrow band Luxeon Star LED, wavelength $635nm$, is used to illuminate an extended object. The extended object is imaged onto a Retiga CCD camera via a Hamamatsu Spatial Light Modulator(SLM) and a DM. The SLM generates zernike aberrations which are created in MatLab. The aberrations are fed to the SLM via the green component of a RGB cable which is connected to a 2nd graphics card port on the control computer.

The resolution of the zernike images created in MatLab are created to match the pixel dimensions of the SLM which is 1024 x 768. The SLM can create a 2π phase change and the phase can be wrapped in the MatLab program to place stronger aberrations in the system.

The deformable mirror is a 37-channel OKO mirror[18] with a diameter of 15mm and has a frequency range of up to 1 KHz. The device can be used for fast dynamic correction of low-order optical aberrations such as defocus, astigmatism, coma, etc. The mirror is operated over a range of 0 to 255 V. The experimental set-up can be seen below in figure 2.

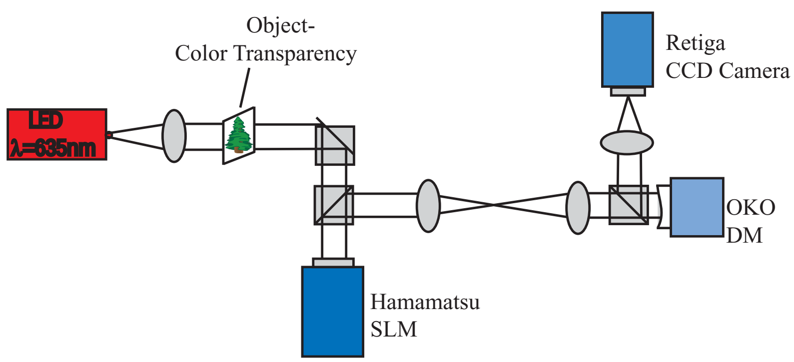

Figure 2. Experimental set-up.

4.2. SLM Aberration Generation

The MatLab program was written to create any combination of zernikes. These aberrations could be 'dialled up' and placed onto the SLM. The phase change created by placing zernike patterns on the SLM was measured using a Fisba interferometer and a selection of aberrations can be seen in figure 3. The images to be corrected were distorted with a combination of defocus and astigmatism. The magnitude of these two aberrations was not fully calibrated over the image plane and the image is further disturbed by system aberrations.

4.3. Experimental Process

With the experimental set-up described above, the power law metric (eq:1) described by Muller and Buffington was examined. This metric was shown to relate low wavefront aberration to an increased sharpness value for extended objects[1].

Various combinations of zernike aberrations were generated and each algorithm was run to correct for the aberrations. The algorithms were tested to maximise the S_1 (eq : 1) sharpness metric for a combination algorithms. The algorithms were also used to test the limit of correction system. This was determined by placing an aberration in the system, running the algorithm to correct for the aberration and subsequently increasing the aberration until the DM/algorithm could not find any corrected solution. In this sense the limitation of correction could be a limitation of either the algorithm or the physical limits of the DM deformation.

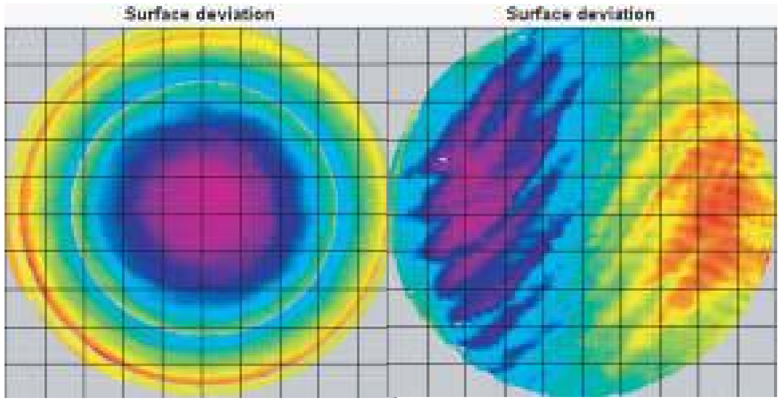

Figure 3. Example of Zernike aberrations generated on SLM, defocus(left 1.5λ P-V) and coma(0.5 λP-V).

5. RESULTS

To compare the correction of aberated extended images a USA AF target image was used. This enabled a profile to be taken through aberrated and corrected images. The results of correction of an unaberrated, aberrated and corrected target image can be seen below in figure 4.

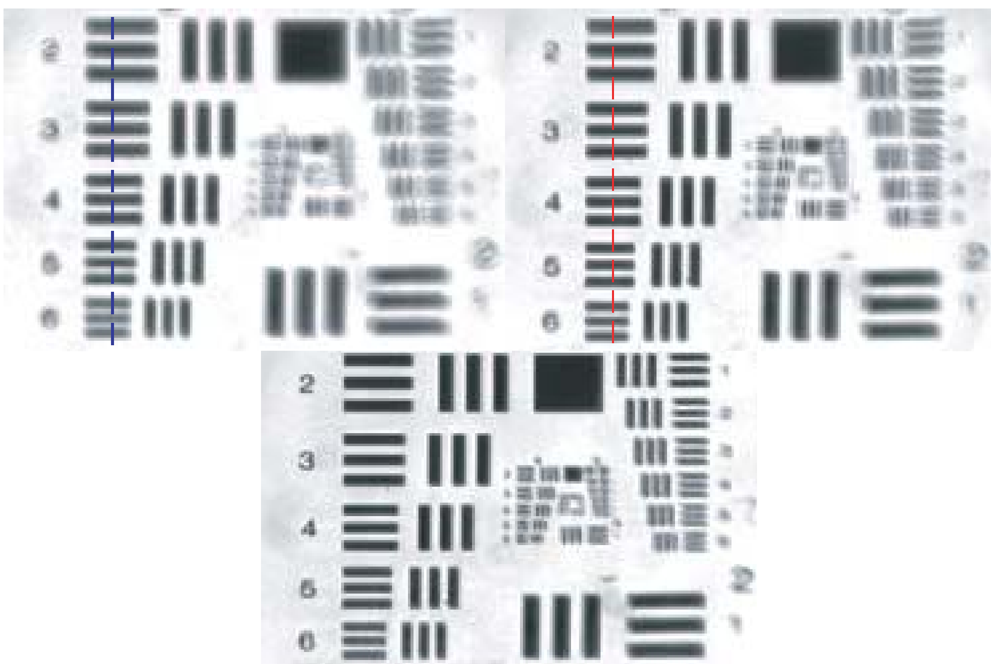

Figure 4. Example of correction achieved with the simplex algorithm with the aberrated image top left, corrected image(1000 iterations of the simplex) top right and unaberrated image bottom.

As can be seen there is a significant degree of correction to the aberated target image. The central bar targets in the image can be resolved better and more detail is present. However, it is clear that the correction is not perfect. It could be the case that simplex algorithm fell into a local minimum or that the aberration was too much for the mirror to correct for, that is, the limited stroke of the mirror can't take the necessary conjugate shape for full correction.

To demonstrate that the image is sharpened and the aberration reduced, a profile is taken through two sections of the target image and the profiles are plotted together, as seen in figure 5.

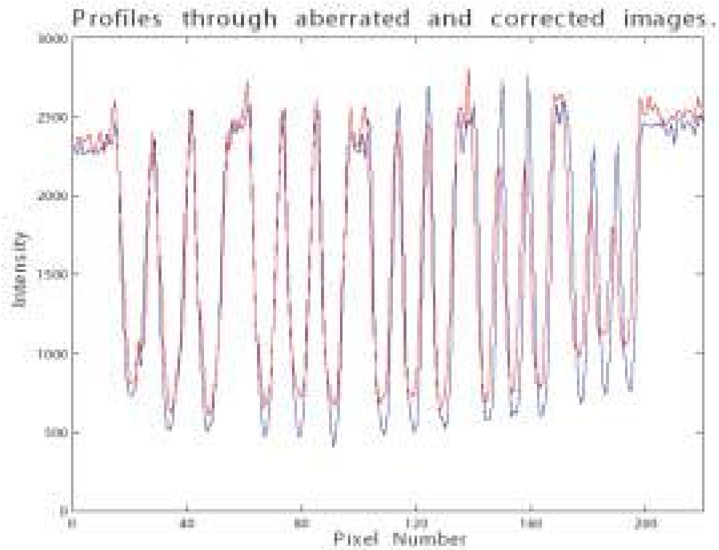

Figure 5. Profiles taken through corrected and uncorrected target images.

The same corrective process was carried out for an aberrated target image with correction being determined by the stochastic non-parallel gradient descent algorithm and the results can be seen in figure 6. As can be seen in figure 7, where the profiles have again been taken in the same region as for the results achieved for the simplex algorithm, good correction is achieved corresponding to an increased contrast in the target image.

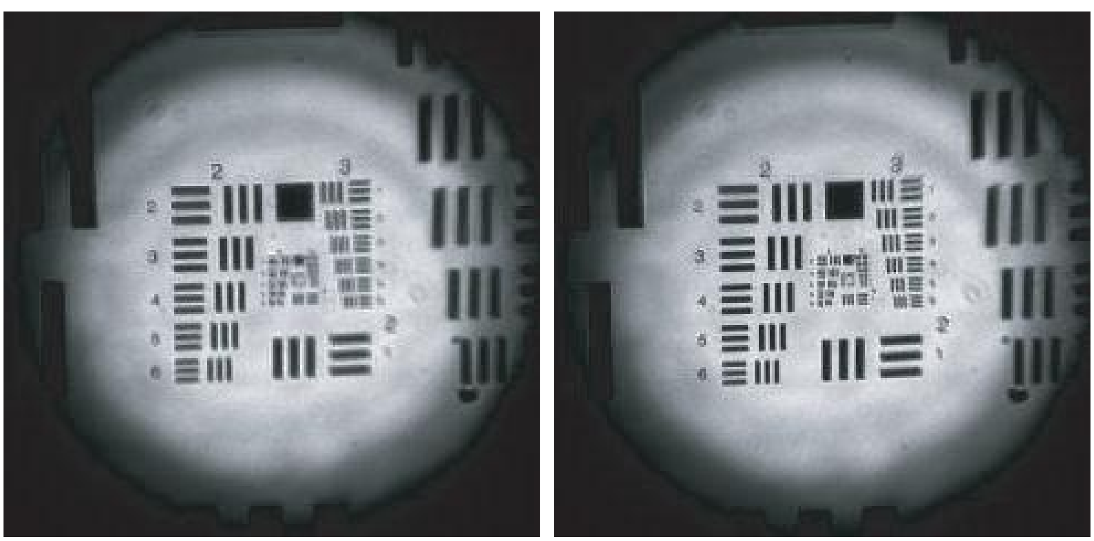

Figure 6. Aberrated(left) and corrected image. Results achieved for SNPGD algorithm.

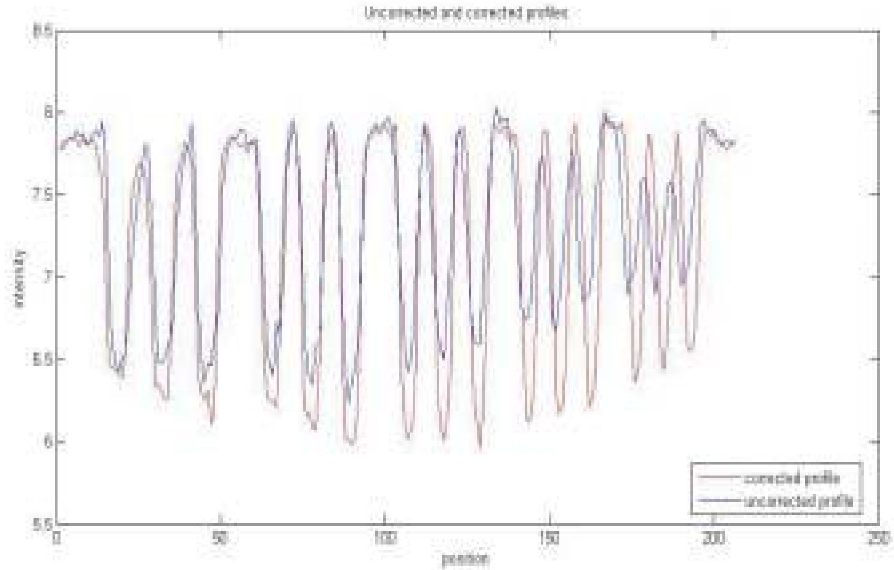

Figure 7. Profile taken through corrected and uncorrected target image for SNPGD algorithm.

It can be seen that the corrected image has much more contrast through the profile. This corresponds to a reduction of the aberrations and an increase in the image sharpness.

The SPGD algorithm was also tested with the same extended object and aberrations and the results shown in figures 8 and 9.

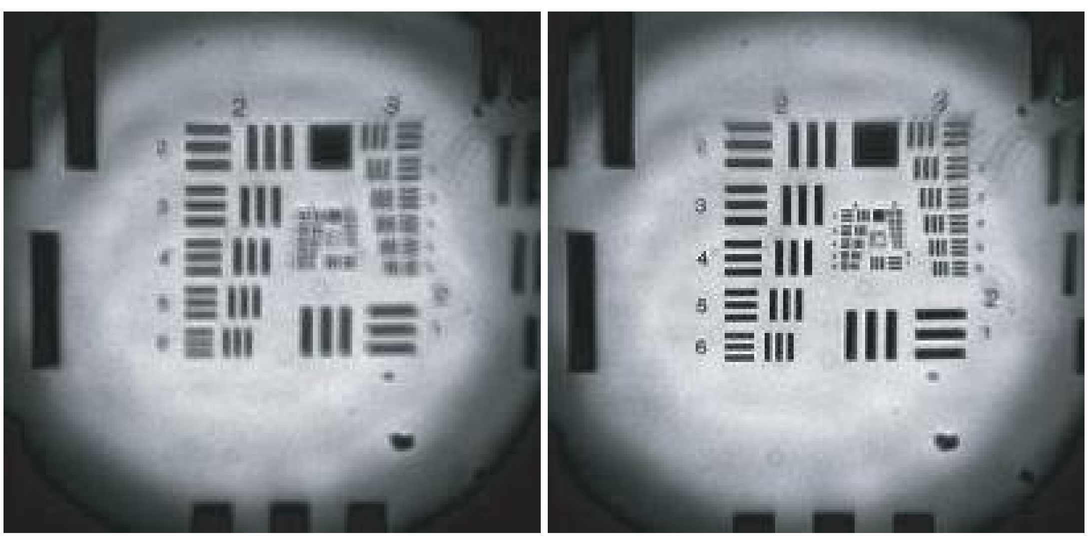

Figure 8. Aberrated and corrected image resulting from SPGD algorithm correction.

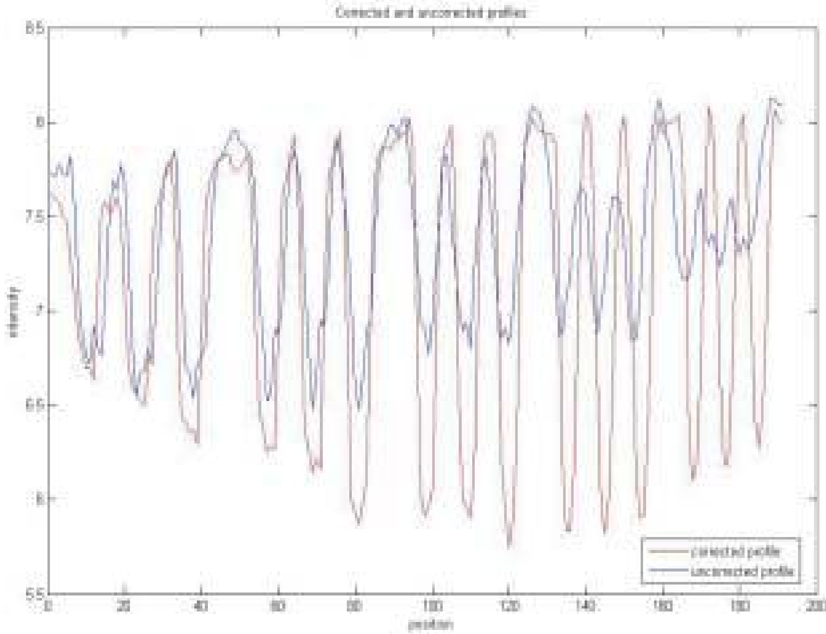

Figure 9. Profiles taken through aberrated and corrected images for SPGD algorithm.

The simulated annealing algorithm, which was also able to correct for aberated images, is, through its nature, a much slower algorithm and typically 10,000 iterations are required to achieve results similar to those achieved by 1000 iterations of the simplex or 100 of the SPGD algorithm. An aberrated and the corresponding corrected image are shown in figure 10. It can be seen that there is greater resolution in the center of the target image. A profile taken through the same target areas as for the previous algorithms can be seen in figure11.

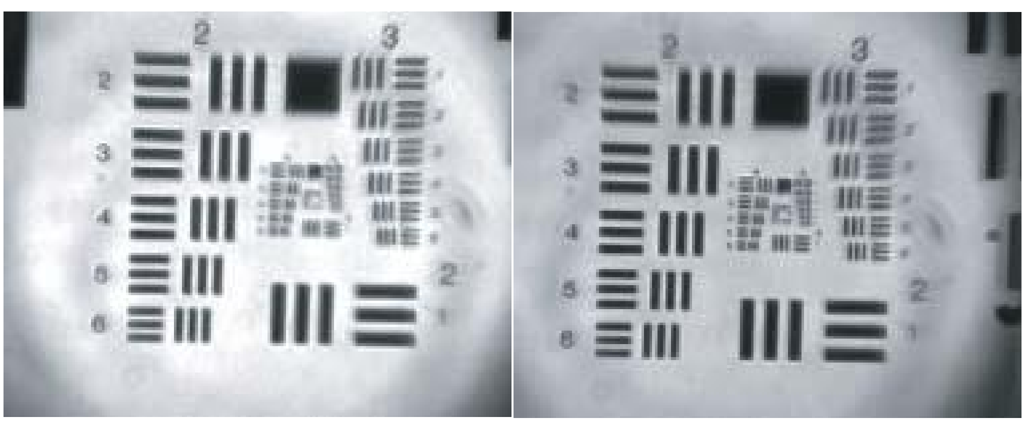

Figure 10. Aberrated(left) and corrected images for a simulated annealing algorithm.

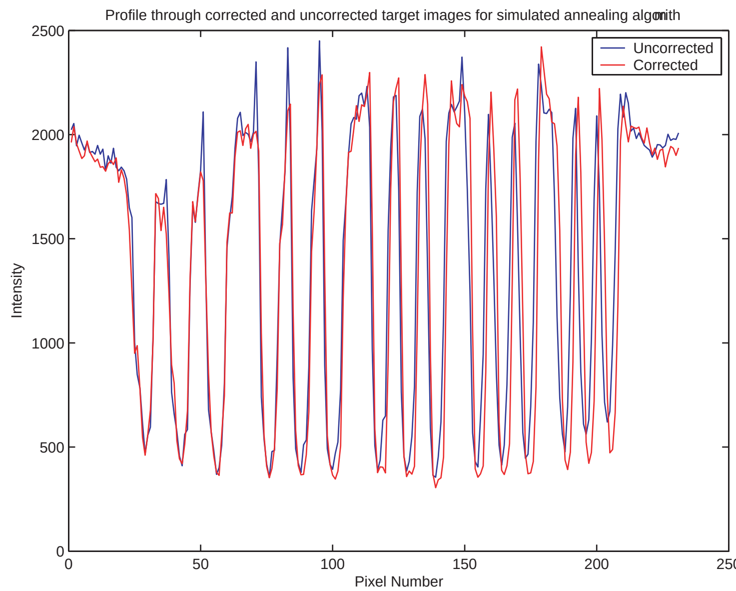

Figure 11. Profiles taken through aberrated and corrected images for the simulated annealing algorithm.

To demonstrate that sharpness maximisation can correct for extended object of varying types the SPGD algorithm was used to correct for an aberrated image of a building. The increased clarity of the writing on the building demonstrates that by maximising the sharpness an aberrated image can be corrected.

Figure 12. Shows aberrated and corrected images from university building.

6. CONCLUSIONS

As mentioned above each algorithm was tested for the S_1 metric for $n = 2$. Preliminary tests were carried out for n=3, n=4 but little difference was noted in the performance of the metrics. Further analysis is needed to determine the performance of these metrics. There are several other sharpness metrics[1] that can be applied to extended objects and these too should be tested to determine which sharpness metric performs best and for what object base.

The power-law metrics set out by Muller and Buffington have been shown to produce good correction for a point source image[2]. This paper shows that the power law metrics can also be applied to extended objects to minimise aberrations.

It has been shown that the power-law metrics can be used to “blindly” correct for small aberrations in an indirect wavefront sensing system, or, act as a wavefront-sensor less correction. Each of the algorithms tested produced good correction to images aberrated by a combination of defocus and astigmatism. They have potential to correct for a combination of zernike aberrations introduced into the system - to the limit of the deformable mirror. Further analysis needs to be made to test the algorithms and the deformable mirror to the limit of their correction.

The SPGD and SGD algorithms were found to achieve the best degree of correction. The simulated annealing algorithm which was an adapted extension of a simplex algorithm base was found to produce corrected results only comparable to the simplex alone. The simulated annealing algorithm requires at least a factor of 10 more iterations than the simplex so in this case was not found to be beneficial. In principle the simulated annealing algorithm should find the global minimum and its apparent failure to do so is a consequence of its initial parameters and this is something that need to examined more closely.

The corrected images displayed in this paper are of USA AF target images but its shown that this doesn’t mean that the algorithms restricted to correcting for such images. The algorithms could correct for aberrated images of scenes taken around the university, as seen in figure?

ACKNOWLEDGEMENTS

This research is funded by Science Foundation Ireland under grant number SFI/01/PL2/B039C and by HP Laboratories.

REFERENCES

1. R. A. Muller and A. Buffington, “*Real-time correction of atmospherically degraded telescope images through image sharpening*”, J Opt. Soc. Am. **67**, 1200-1210 (1974).
2. L. P Murray, J. C. Dainty and E. Daly, “*Wavefront correction through image sharpness maximisation*” Proc. SPIE Vol. 5823 p.40-47 Jun. 2005
3. J. A. Nelder and R. Mead. “*A simplex method for function minimisation*” Computer Journal, 7:308, 1965.
4. R. K. Tyson, “*Principles of Adaptive Optics*”, Academic Press, 2nd Edition, 1998.
5. J. W. Hardy, “*Adaptive Optics for Astronomical Telescopes*”, Oxford University Press, 1998.
6. H. W. Babcock, “*The possibility of compensating astronomical seeing*”, Publ. Astro. Soc. Pac. **65**, 229-236 (1953)
7. V. I. Polejaev and M. A. Vorontsov, “*Adaptive active imaging system based on radiation focusing for extended targets*”, SPIE Proc., Vol. 3126, 1997.
8. J. R. Feinup, J. J. Miller, “*Aberration correction by maximising generalised sharpness metrics*”, Publ. J.O.S.A. Vol. **20**, 4, 609-620, 2003.
9. M. A. Vorontsov, “*Image quality criteria for an adaptive imaging system based on statistical analysis of the speckle field*”, J.O.S.A. Vol. **13**, 7, 1456-1466, 1996.
10. M. Cohen, G. Cauwenbergs and M. A. Vorontsov, “*Image sharpness and beam focus VLSI sensors for AO*”, IEEE Sensors, Vol. **2**, 6, 2002.
11. M. A. Vorontsov, A. V. Koriabin and V. I. Shmalausen, “*Controlling Optical Systems*” (Nauka, Moscow, 1998)
12. N. Doble, “Image Sharpening Metrics and Search Strategies for Indirect Adaptive Optics”, Thesis submitted to the University of Durham, 2000.
13. J. A. Nelder and R. Mead, “*A simplex method for function minimisation*”, Computer Journal 7, 308-313, 1965.
14. J. C. Lagarias, J. A. Reeds, M. H. Wright and P. E. Wright, “*Convergence properties of the Nelder-Mead Simplex Method in low dimensions*”, SIAM J. Optim., Vol. **9**, No. 1, 112-147, 1998.
15. M. A. Vorontsov et al, “*Adaptive imaging system for phase-distorded extended source and multiple-distance objects*”, Applied Optics, Vol. 36, No. 15, 3319-3328, 1997
16. S.Kirkpatrick and C. D. Gelatt and M. P. Vecchi, “*Optimization by Simulated Annealing*”, Science, Vol 220, Number 4598, pages 671-680, 1983.
17. W. H. Press, S. A. Teukolsky, W. T. Vetterling and B. P. Flannery. Numerical Recipies in C: Second Edition. Cambridge University Press, Cambridge, 1992.
18. http//okotech.com